

Spin-charge separation in the single hole doped Mott antiferromagnet

Z.Y. Weng,^a V.N. Muthukumar,^b D.N. Sheng,^{a,c} C.S. Ting^a

^aTexas Center for Superconductivity, University of Houston, Houston, TX 77204-5506

^bJoseph Henry Laboratories of Physics, Princeton University, Princeton, NJ 08544

^cDepartment of Physics and Astronomy, California State University, Northridge, CA 91330

The motion of a single hole in a Mott antiferromagnet is investigated based on the $t - J$ model. An exact expression of the energy spectrum is obtained, in which the irreparable phase string effect [Phys. Rev. Lett. **77**, 5102 (1996)] is explicitly present. By identifying the phase string effect with spin backflow, we point out that spin-charge separation must exist in such a system: the doped hole has to decay into a neutral spinon and a spinless holon, together with the phase string. We show that while the spinon remains coherent, the holon motion is deterred by the phase string, resulting in its localization in space. We calculate the electron spectral function which explains the line shape of the spectral function as well as the “quasiparticle” spectrum observed in angle-resolved photoemission experiments. Other analytic and numerical approaches are discussed based on the present framework.

71.27.+a, 74.20.Mn, 74.72.-h

I. INTRODUCTION

Since the discovery of high- T_c superconductivity, there has been much effort to elucidate the properties of doped Mott insulators. In this context, the specific case of one hole in a Mott insulating antiferromagnet (half filled band) has been the subject of extensive theoretical and experimental investigation. These studies address the basic question, whether the motion of a hole in the antiferromagnet can possibly be described within a quasiparticle approach. Photoemission spectroscopy provides valuable information that can help resolve this issue. Experimental results from angle resolved photoemission spectroscopy (ARPES) are now available for $\text{Sr}_2\text{CuO}_2\text{Cl}_2$ as well as for $\text{Ca}_2\text{CuO}_2\text{Cl}_2$ [1–5]. Both these materials are Mott insulators and are parent compounds of the high- T_c cuprates. The results from ARPES can be summarized as follows: (i) the spectral features observed are *not* sharp at all. Quite to the contrary, an intrinsic broad feature extending to energies of the order of 1.5 eV before merging into the main valence band is seen. This is to be contrasted with sharp spectral features that one expects in a quasiparticle scenario; (ii) the observed dispersion is isotropic around $\mathbf{k}_0 = (\pi/2, \pi/2)$; (iii) the measurements of Ronning *et al.* [3] reveal the presence of a so-called remnant Fermi surface of the momentum structure in the energy-integrated spectral function.

The broad spectral features seen in ARPES strongly suggest the breakdown of the quasiparticle picture. Based on such considerations, Laughlin [6] conjectured the failure of quasiparticle theory in these materials, and further proposed, that the observed isotropic dispersion has its origins in an underlying spinon spectrum. This picture envisages spin-charge separation with the scale of the observed dispersion determined by the superexchange J .

An entirely different picture is presented by the self-consistent Born approximation (SCBA) approach [7–10]. Though this scheme is based on the $t - J$ model, it depicts a spin-polaron picture for the single hole case where the doped hole behaves not very different from a quasiparticle in the Landau-Fermi liquid theory. The SCBA results have also been supported by exact numerical calculations on finite lattices [11] up to 32 sites [12] as well as variational calculations on larger lattices [13]. Here, the consistency amongst different numerical methods mostly concerns the spectrum $\epsilon_{\mathbf{k}}$, usually defined as the *minimum* energy for a given momentum \mathbf{k} . The spectrum is *anisotropic* around the “Fermi points” $\mathbf{k}_0 = (\pm\pi/2, \pm\pi/2)$ in all these calculations. It is called a “quasiparticle” spectrum since a sharp peak in the spectral function usually appears at $\epsilon_{\mathbf{k}}$ in both the SCBA as well as results from exact diagonalization. Note that these results are *not* consistent with ARPES which exhibits an *isotropic* dispersion around \mathbf{k}_0 , and rather broad spectral features. Thus, to account for the former, the inclusion of second (t') and third (t'') nearest neighbor hoppings to the $t - J$ model have been proposed in the literature [2,14–16]. However, this approach is meaningful only when the quasiparticle description holds, *i.e.*, only if a sharp quasiparticle peak exists at $\epsilon_{\mathbf{k}}$ in the $t - J$ model. As illustrated in Fig. 1, if in the thermodynamic limit, the spectral function for a given momentum \mathbf{k} does not show a sharp quasiparticle peak, then, notwithstanding how accurately $\epsilon_{\mathbf{k}}$ is determined by various theoretical methods, it has no experimental implication. For, in this case, the higher energy $\epsilon'_{\mathbf{k}}$ at the broad “peak” in Fig. 1, which is observable experimentally, may have nothing to do with the anisotropic $\epsilon_{\mathbf{k}}$.

On more general grounds, the breakdown of the Landau-Fermi quasiparticle picture has been discussed by Anderson for a doped Mott insulator in the presence of an upper Hubbard band [17]. He argues that the quasiparticle weight

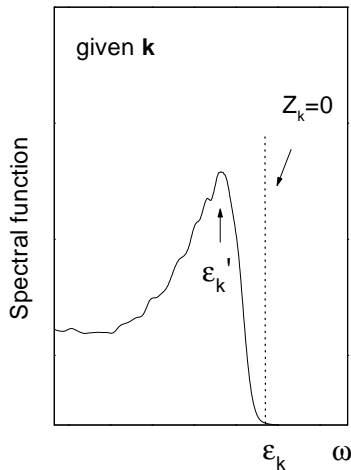


FIG. 1. Schematic illustration of a spectral function at a given \mathbf{k} in which the quasiparticle weight $Z_{\mathbf{k}} = 0$ at the energy bottom $\epsilon_{\mathbf{k}}$. Here the “quasiparticle” peak at $\epsilon'_{\mathbf{k}}$ has nothing to do with the Landau-Fermi quasiparticle.

Z vanishes due to unrenormalizable Fermi-surface phase shifts induced when a particle is injected into the Mott insulator. Indeed, based on a rigorous formulation of the single-electron Green’s function in the one-hole case using the $t - J$ model, it has been demonstrated [18,19] that the quasiparticle weight Z at the Fermi surface must vanish in the thermodynamic limit due to the presence of the phase string effect. Such a phase string effect can be considered as the equivalent of the phase shifts proposed by Anderson in the Hubbard model.

This paper concerns the effect of the aforementioned phase string on the dynamics of a single hole introduced in an antiferromagnet. We show how the phase string leads to the frustration of kinetic energy of the hole. We then show that the phase string effect is related to spin-charge separation and that the charge carrier is actually a spinless holon. We find that the holon propagator is localized in space, owing to the phase string. This is in contrast to the prediction of SCBA that the hole behaves as a Landau quasiparticle. Our result for the holon propagator is consistent with an earlier conclusion that the quasiparticle weight is zero for the doped hole [18,19]. It does not necessarily contradict finite-size calculations, as the localization length scale turns out to be much larger than typical sample sizes in numerical studies. We find the only coherent object to be a neutral spinon excitation created by the doped hole whose energy spectrum is responsible for an isotropic “quasiparticle” dispersion. Thus, our results provide a natural explanation of the ARPES results and support the conjecture made in Ref. [6]. We also discuss how the observed line shapes reflect spin-charge separation, and finally, in the Appendix, how the remnant Fermi surface structure may be understood as a peculiar consequence of the phase string effect at higher energies.

II. PHASE STRING: THE KEY EFFECT INDUCED BY THE MOTION OF A HOLE

In this section, we examine the effects induced by the motion of a single hole in an antiferromagnetic background. In Sec. IIA, we shall review a few basic results of the slave-fermion formalism. We then go on to discuss the effect of the phase string on the kinetic energy of the hole, spin-charge separation and the localization of the holon due to the phase string.

A. Slave-fermion formalism of the $t - J$ model

We begin with the slave-fermion representation $c_{i\sigma} = f_i^\dagger b_{i\sigma} (-\sigma)^i$ [20] and express the $t - J$ model $H_{t-J} = H_t + H_J$ in the following form:

$$H_J = -\frac{J}{2} \sum_{\langle ij \rangle} (\hat{\Delta}_{ij}^s)^\dagger \hat{\Delta}_{ij}^s \quad (2.1)$$

with

$$\hat{\Delta}_{ij}^s = \sum_{\sigma} b_{i\sigma} b_{j-\sigma} \quad , \quad (2.2)$$

and

$$H_t = -t \sum_{\langle ij \rangle} \hat{B}_{ij} f_i^{\dagger} f_j + h.c. \quad , \quad (2.3)$$

with

$$\hat{B}_{ij} = \sum_{\sigma} \sigma b_{j\sigma}^{\dagger} b_{i\sigma} \quad . \quad (2.4)$$

At half-filling, the bosonic resonating-valence-bond (RVB) description given by Liang, Doucot, and Anderson [22] has provided by far, the most accurate picture (see Fig. 2) for both long-range as well as short-range antiferromagnetic (AF) correlations in two dimensions (2D). In this theory, it is found [22,23] that the long-range AF correlations, including the AF long-range order (AFLRO) occurring in the thermodynamic limit, constitute only a *small* fraction of the ground-state energy and the dominant contribution mainly comes from the *short-range* RVB correlations. Thus, the ground state at half-filling may be regarded as AFLRO + RVB, of which, AFLRO is the most vulnerable part easily removed by either temperature or doping with little energy cost. The mean-field version of this bosonic RVB description is known as the Schwinger-boson mean-field theory (SBMFT) [24]. This theory works quite well at half-filling, and is characterized by a bosonic RVB order parameter

$$\Delta^s = \langle \hat{\Delta}_{ij}^s \rangle \neq 0 \quad . \quad (2.5)$$

But away from half-filling, the problem is highly nontrivial. The reason can be attributed to the fact that the hopping integral $\langle \hat{B}_{ij} \rangle = 0$ in H_t . This is generally true due to the sign σ appearing in (2.4). So the motion of the hole will be very sensitive to how the spin backflow \hat{B}_{ij} is treated which is a non-perturbative problem and is the key issue to be dealt with in the present work.

In SCBA approach [7–10], the hole can acquire some kinetic energy through the *dynamic fluctuations* of \hat{B}_{ij} . In this approach, only the long wavelength fluctuations associated with AFLRO is considered, where \hat{B}_{ij} is approximated in large- S (spin wave) expansion [8] by

$$\hat{B}_{ij} \approx \hat{B}_{ij}^{LSW} = b_0 \sum_{\sigma} \sigma \left[b_{j\sigma}^{\dagger} + b_{i\sigma} \right] , \quad (2.6)$$

in which b_0 denotes the condensed part of the Schwinger boson field, corresponding to AFLRO [25]. Now, the hopping of the hole is assisted by the fluctuations of \hat{B}_{ij}^{LSW} . This is the idea behind the SCBA, and within this approach it has been found that the hole behaves just like a Landau quasiparticle, known as the spin-polaron, with four Fermi points at $\mathbf{k}_0 = (\pm\pi/2, \pm\pi/2)$ [7–10]. We reemphasize that within this approximation only the *long-wavelength* fluctuations associated with AFLRO are involved, and the dominant *short-range* RVB correlations, which are independent of AFLRO characterized by $b_0 \neq 0$, are completely neglected.

The validity of the SCBA approach is based on the presumption that spin mismatches, described by the spin backflow \hat{B}_{ij} induced by the hopping of the hole, can be repaired through spin flip process in H_J . Thus, the final

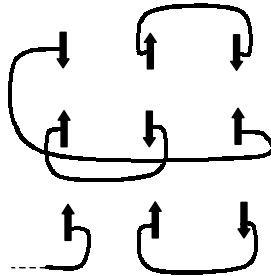


FIG. 2. The resonating-valence-bond picture [22,23] of bosonic spins provides a highly accurate description of both short-range and long-range antiferromagnetic spin correlations in the Heisenberg model.

state of the hole, after traversing a closed path through the antiferromagnetic background, is identical to its initial state. This would be true if one focuses only on, say, the \hat{z} -component of the spins. But since we are dealing with a quantum spin system in which each spin has three components that do not commute with one another, there will actually be three components in the spin mismatches induced by the motion of the hole. For the spin-1/2 case, it has been explicitly proven [18] that such string-like spin defects *cannot* be simultaneously repaired through H_J . Once the spin configuration (*i.e.*, the \hat{z} -component) disordered by the hole hopping is restored by spin flips at low energy, a string defect in the transverse components remains, which is described by a sequence of signs in the quantum description of the hole. This defect is called the phase string [18]. The effect of this phase string, as we shall see in the following two subsections, manifests itself both in the expression for the kinetic energy of the hole as well as its propagator.

B. Effect of the phase string on the energy of the hole

In this section, we shall demonstrate that the total energy at momentum \mathbf{k} for the one-hole case can be exactly formulated as

$$E_{\mathbf{k}} = E_0 - \frac{t}{N} \sum_{ij} e^{i\mathbf{k}\cdot(\mathbf{r}_i - \mathbf{r}_j)} M_{ij} \quad , \quad (2.7)$$

where

$$M_{ij} \equiv \sum_{\{c\}\{\phi\}} M[c; \{\phi\}] (-1)^{N_c^\downarrow} \quad . \quad (2.8)$$

Here, E_0 denotes the spin ground-state energy with the hole being *fixed* at a given lattice site. The energy gain due to the hopping arises solely from the second term. In the expression for M_{ij} , the summations run over all the possible paths of the hole connecting i and j , $\{c\}$, as well as spin configurations, $\{\phi\}$. The weight functional M is positive semi-definite,

$$M[c; \{\phi\}] \geq 0 \quad (2.9)$$

such that the phase factor $(-1)^{N_c^\downarrow}$ is “uncompensated” in (2.8). Here N_c^\downarrow counts the total number of \downarrow spins (or \uparrow spins by symmetry) being *exchanged* with the hole moving along the path c . As illustrated in Fig. 3, $(-1)^{N_c^\downarrow} = \dots(+1) \times (-1) \times (-1) \times \dots$ is the phase string on the path c , which was first identified in the exact formulation of the single-electron Green’s function [18]. Later we shall see that, owing to the factor $(-1)^{N_c^\downarrow}$, the lowest energy of $E_{\mathbf{k}}$ is obtained for $\mathbf{k} = \mathbf{k}_0$, consistent with numerical calculations [11–13].

From (2.7), (2.8) and (2.9), we come to an important conclusion. Without the phase string factor $(-1)^{N_c^\downarrow}$, the total energy would certainly be *lower* (as $M \geq 0$). Thus, $(-1)^{N_c^\downarrow}$ represents the frustration on the kinetic energy of the hole. This effect is (i) *irreparable* as no other signs can be generated from the spin background to compensate it; (ii) *singular* since a change of N_c^\downarrow by ± 1 will lead to a maximal change in $(-1)^{N_c^\downarrow}$; and (iii) thus expected to dominate the low energy dynamics of the hole. A similar effect is well known in fermionic systems where each fermion’s path is also weighted by a “phase string” determined by the number of fermions “exchanged” with it. The difference in this case is that the “exchange” is between two *different* species, the hole and spins. Therefore, such a phase string effect implies an intrinsic *mutual statistics* between these two degrees of freedom [19].

The proof of (2.7)-(2.9) is straightforward. We use the Wigner-Brillouin formula,

$$E_{\mathbf{k}} = E_0 + \langle \Phi_0(\mathbf{k}) | [H_t + H_t G_J(E_{\mathbf{k}}) H_t + \dots]' | \Phi_0(\mathbf{k}) \rangle \quad , \quad (2.10)$$

where $G_J(E) \equiv 1/(E - H_J)$ and $[\dots]'$ excludes $|\Phi_0\rangle$ as the intermediate state. Here $|\Phi_0(\mathbf{k})\rangle = 1/\sqrt{N} \sum_i e^{i\mathbf{k}\cdot\mathbf{r}_i} |\Phi_0^{(i)}\rangle$ with $|\Phi_0^{(i)}\rangle$ denoting the ground state of H_J with the hole localized at a site i , *viz.*, $H_J |\Phi_0^{(i)}\rangle = E_0 |\Phi_0^{(i)}\rangle$. One can expand $|\Phi_0^{(i)}\rangle$ in terms of the complete spin-hole basis $\{|\phi; (i)\rangle\}$ (ϕ being a spin configuration with the hole at site i) as $|\Phi_0^{(i)}\rangle = \sum_{\phi} \chi_{\phi}^i |\phi; (i)\rangle$. As shown in Ref. [18,19], $\chi_{\phi}^i \geq 0$, which means that the Marshall sign rule [21] still applies to the doped ground state *if* the hole is not moving. By inserting the complete set of basis states and following the steps outlined in [18] for calculating the single-hole propagator, one can easily obtain (2.7), with the weight functional

$$M[c; \{\phi\}] = \chi_\phi^i \chi_{\phi'}^j \prod_{s=1}^{K-1} \langle \phi^{s+1}; (m_s) | \hat{P} G_J(E_{\mathbf{k}}) \hat{P} | \phi^s; (m_s) \rangle (-t) \quad , \quad (2.11)$$

in which ϕ^s and ϕ^{s-1} correspond to spin configurations in intermediate states, and the hole site m_s is on a path c connecting two arbitrary sites i and j : $m_0 = i, m_1, \dots, m_K = j$ ($\phi^0 \equiv \phi, \phi^K \equiv \phi'$). Following Ref. [18], we can show that $\langle \phi^s; (m_s) | \hat{P} G_J(E) \hat{P} | \phi^{s-1}; (m_s) \rangle \leq 0$ as long as $E < E_0$ (note that the projection operator $\hat{P} = 1 - |\Psi_0\rangle\langle\Psi_0|$ has no effect in the thermodynamic limit $N \rightarrow \infty$). Since we are interested in low energy states $E_{\mathbf{k}} < E_0$, the weight functional M in (2.11) is always positive semi-definite.

C. Phase string effect and spin-charge separation

In the above subsection, we showed that the phase string manifests itself as irreparable sign (phase) frustrations induced by the hole motion. In this section, we shall establish an intrinsic connection between such a phase string and spin-charge separation.

To this end, let us first consider the origin of the phase string factor $(-1)^{N_c^\downarrow}$ in (2.8). Equation (2.4), defining \hat{B}_{ij} , can be rewritten as

$$\hat{B}_{ij} = (B_{ij}^0) e^{i\hat{\phi}_{ij}} \quad , \quad (2.12)$$

where

$$B_{ij}^0 = \sum_{\sigma} b_{j\sigma}^\dagger b_{i\sigma} \quad , \quad (2.13)$$

and

$$\hat{\phi}_{ij} = \pm(\pi/2)[1 - \sigma_{ij}] \quad . \quad (2.14)$$

Here $\sigma_{ij} = 1(-1)$, if an $\uparrow(\downarrow)$ spinon is *exchanged* with the holon at the link (ij) . For products around consecutive links enclosing a loop Γ ,

$$\prod_{\Gamma} \hat{B}_{ij} \hat{B}_{jk} \dots \hat{B}_{li} = \left(\prod_{\Gamma} B_{ij}^0 B_{jk}^0 \dots B_{li}^0 \right) e^{i \sum_{\Gamma} \hat{\phi}} \quad , \quad (2.15)$$

with

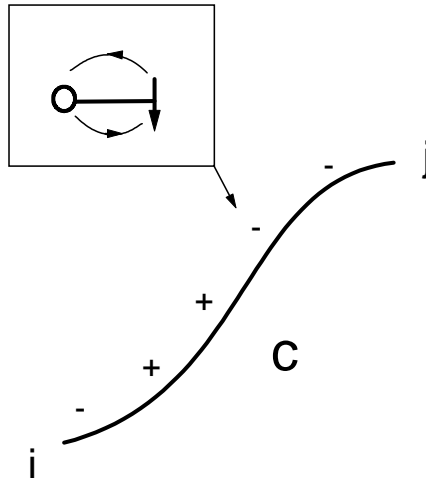


FIG. 3. Phase string as a sequence of signs on the hole path c , determined by the index of each spin exchanged with the hole at every step of hopping.

$$e^{i \sum_{\Gamma} \hat{\phi}} \equiv e^{i[\hat{\phi}_{ij} + \hat{\phi}_{jk} + \dots + \hat{\phi}_{li}]} = (-1)^{N_{\Gamma}^{\downarrow}} , \quad (2.16)$$

where N_{Γ}^{\downarrow} denotes the total number of \downarrow spins *exchanged* with the hole along the loop Γ . Thus, the phase $\hat{\phi}_{ij}$ of the spinon backflow operator (2.12) is the source of the phase string factor in (2.8). This is illustrated by the inset in Fig. 3.

Since the ground state satisfies the Marshall sign rule [21], it is easy to see that

$$\left\langle \prod_{\Gamma} B_{ij}^0 B_{jk}^0 \dots B_{li}^0 \right\rangle_{\text{half-filling}} > 0 . \quad (2.17)$$

(Note that the Marshall sign is totally gauged away in the definition of $b_{i\sigma}$ by the sign factor $(-\sigma)^i$ in the slave-fermion decomposition [19].) This is of course consistent with the previous conclusion that the nontrivial phases in the low-energy states all come from the phase string. A hole slowly hopping around the loop Γ will then acquire a Berry's phase Φ_{Γ} given by

$$\begin{aligned} \Phi_{\Gamma} &= \text{Im} \ln \left\langle \prod_{\Gamma} \hat{B}_{ij} \hat{B}_{jk} \dots \hat{B}_{li} \right\rangle_{\text{half-filling}} \\ &= \text{Im} \ln \left\langle e^{i \sum_{\Gamma} \hat{\phi}} \right\rangle_{\text{half-filling}} . \end{aligned} \quad (2.18)$$

So the phase string effect generally leads to a nontrivial Berry's phase picked up by the hole, as opposed to the quasiparticle picture (of SCBA, for instance) in which the states of the hole before and after traversing a closed path are identical.

Now that we have established the connection between the *phase string effect* and the *spinon backflow*, we are in a position to discuss spin-charge separation. Let us initially suppose that the hole behaves like a quasiparticle with both charge and spin quantum numbers. This means that the holon and spinon should be confined together. In this case totally one \uparrow (\downarrow) spinon will have to be effectively “transferred” back from the final location of the hole to the initial location to ensure a precise spin quantum number \downarrow (\uparrow) being transported with the hole. It then requires that at each step of the holon hopping, the spinon backflow is fully *polarized*, only to involve a \uparrow (\downarrow) spinon being “transferred” backward. Otherwise, since the spinon backflow or the phase string effect cannot be “repaired”, any local fluctuations of the spin polarization of the backflow spinons, no matter how weak they are, will be accumulated to become *arbitrarily* large at a sufficiently long path to *invalidate* that the hole carries a precise spin quantum number $s = 1/2$. In other words, for the spin-charge confinement picture to hold, one must find that $N_c^{\downarrow} = 0$, or, = the total number of links on any path c , such that the phase string factor $(-1)^{N_c^{\downarrow}}$ becomes *trivial* no matter how long the path is. But based on (2.11) one can easily rule out such a scenario, which imposes the extreme restriction that the probability for any other choices of N_c^{\downarrow} vanishes, since an equal probability for both kinds of spinon backflow is explicitly given in the hopping term (2.3). In fact, an analysis [18,19] of the weight functional in the single-electron Green's function has already lead to the conclusion that the phase string effect must be *nontrivial* (which actually causes the spectral weight Z vanish as shown in Refs. [18,19]).

Therefore, *the irreparable nontrivial phase string effect directly leads to a true spin-charge separation in the single-hole doped Mott antiferromagnet*. It confirms the conjecture made by Anderson [17]. We note that spin-charge separation has also been discussed in some exact diagonalization approaches for momenta close to $(0, \pi)$ [15,16]. In the following, we will go a step further and discuss some unique features associated with spin-charge separation.

Let us define the holon propagator G_h in energy space, $G_h(E) \equiv \langle f_j G(E) f_i^{\dagger} \rangle_{\text{half-filling}}$, where $G(E) = 1/(E - H_{t-j})$. On expanding in terms of H_t , $G(E) = G_J + G_J H_t G_J + \dots$, we get

$$\begin{aligned} G_h(j, i; E) &= \sum_{\{c\}} \left\langle \left[\prod_{s=1}^K G_J(-t) \hat{B}_{m_s m_{s-1}} \right] G_J \right\rangle_{\text{half-filling}} \\ &= \sum_{\{c\} \{\sigma_s\}} \left\langle \hat{S}_c(\{\sigma_s\}) \right\rangle_{\text{half-filling}} (-1)^{N_c^{\downarrow}} , \end{aligned} \quad (2.19)$$

where $\hat{S}_c(\{\sigma_s\}) \equiv \left(\prod_{s=1}^K G_J(-t) \left[b_{m_{s-1} \sigma_s}^{\dagger} b_{m_s \sigma_s} \right] \right) G_J$ with $N_c^{\downarrow} = \sum_s (1 - \sigma_s)/2$. In (2.19), c denotes a path connecting two sites i and j , and m_s in the definition of \hat{S}_c is a lattice site on any path c . As with the the positive semi-definite

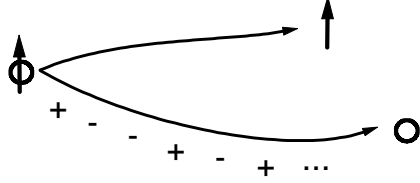


FIG. 4. Spin-charge separation in the single-hole case: the injected hole decays into a neutral spinon and a spinless holon, and the holon will pick up the full effect of phase string. Representing the spinon backflow effect, the irreparable phase string ensures spin-charge separation as discussed in the text.

functional M in the expression (2.8) for $E_{\mathbf{k}}$, one can easily prove that $\langle \hat{S}_c \rangle \geq 0$ for energies $E < E_0$. This means that there are no other sources of phases at low energies to repair the phase string factor $(-1)^{N_c^\downarrow}$. It should be noted that *the single-electron* Green's function for the one-hole case has been exactly formulated previously in a very similar fashion [18]. There, it was found that each hole path is also modulated by the same phase string $(-1)^{N_c^\downarrow}$. This result taken in conjunction with (2.19), shows that *the effect of the phase string is entirely in the holon sector*, while the spinon released from the hole is not directly associated with such phase frustrations. Such a picture is shown in Fig. 4. This is not entirely surprising, as we do not expect the motion of a single hole to affect the (thermodynamically large) spin subsystem, except possibly at short time scales or high energies.

D. Localization of the holon due to the phase string effect

Thus far, we have discussed the general properties of the phase string effect in a rigorous form. To further study the one-hole problem in a quantitative way, we need a suitable framework for approximation. As mentioned earlier, the mean field version of the bosonic RVB theory (SBMFT) provides [24] a fairly good description of the undoped antiferromagnet. We now assume, consistent with the discussion so far, that the presence of one hole does not alter the low energy properties of the spin subsystem as the irreparable phase string is to be solely picked up by the hole. In the following we shall discuss a direct consequence of the phase string effect on the charge part within this approximation: the localization of the holon.

At half-filling, SBMFT characterized by (2.5) is described by the Bogoliubov transformation [24]

$$b_{i\sigma} = \frac{1}{\sqrt{N}} \sum_{\mathbf{k}} \eta_{\mathbf{k}\sigma} e^{i\sigma\mathbf{k}\cdot\mathbf{r}_i} \left[u_{\mathbf{k}} \gamma_{\mathbf{k}\sigma} - v_{\mathbf{k}} \gamma_{\mathbf{k}-\sigma}^\dagger \right], \quad (2.20)$$

where $\gamma_{\mathbf{k}\sigma}^\dagger$ is an operator that creates an elementary spinon excitation with a gapless spectrum at $T = 0^+$,

$$E_{\mathbf{k}}^s = 2.32J \sqrt{1 - \xi_{\mathbf{k}}^2}, \quad (2.21)$$

and $u_{\mathbf{k}} = 1/\sqrt{2}(2.32J/E_{\mathbf{k}}^s + 1)^{1/2}$, $v_{\mathbf{k}} = 1/\sqrt{2}(2.32J/E_{\mathbf{k}}^s - 1)^{1/2} \text{sgn}(\xi_{\mathbf{k}})$, with $\xi_{\mathbf{k}} = (\cos k_x + \cos k_y)/2$. Within this mean field theory, it is easy to verify that $\langle b_{i\uparrow}^\dagger b_{j\uparrow} \rangle = \langle b_{i\downarrow}^\dagger b_{j\downarrow} \rangle \equiv 0$. If we use this result naively, when there are $N - 1$ spins (and a hole), we would conclude (erroneously) that $B^0 = \langle B_{ij}^0 \rangle = 0$, namely, the amplitude of the hopping integral vanishes. This is incorrect because the hopping term connects two spin subspaces, corresponding to the hole at site i and j , respectively, which are not necessarily identical in symmetry. This subtlety has to be incorporated in any calculation, as will be done below.

As a first step, let us go back to the case of half filling. Here, it is important to recognize that the factor $\eta_{\mathbf{k}\sigma}$ in (2.20) which satisfies $\eta_\sigma = \eta_{-\sigma}^*$ and $|\eta| = 1$ cannot be completely determined at the level of mean field theory; *i.e.*, the mean field order parameter $\langle b_{i\sigma} b_{j-\sigma} \rangle$ is independent of the choice of $\eta_{\mathbf{k}\sigma}$. Therefore, there is a hidden symmetry in SBMFT, which is related to the exact local particle-hole invariance of the system as to be discussed later.

We now exploit this symmetry in SBMFT for the case when there is one hole. Fixing the position of the hole, one may define a subspace for the spins, which, at the level of mean field theory, is again described by the Bogoliubov transformation (2.20). It should be remembered that equation (2.20) now describes an $N - 1$ spin subspace. By

choosing $\eta_{\mathbf{k}\sigma} = [-\text{sgn}(\xi_{\mathbf{k}})]^{k_h}$, where $k_h = 0$ if the hole is on the even sublattice and $k_h = 1$ if the hole is on the odd sublattice site, one has $\eta_{\mathbf{k}\sigma} \rightarrow -\text{sgn}(\xi_{\mathbf{k}})\eta_{\mathbf{k}\sigma}$ when the hole hops between the sublattices [26]. Then noting that in B_{ij}^0 , $b_{j\sigma}^\dagger$ and $b_{i\sigma}$ belong to two different spin subspaces, one obtains

$$B^0 = \frac{2}{N} \sum_{\mathbf{k} \neq 0} |\xi_{\mathbf{k}}| v_{\mathbf{k}}^2 \approx 0.4 \quad . \quad (2.22)$$

It is easy to verify that the above choice of $\eta_{\mathbf{k}\sigma}$ optimizes B^0 . Thus, we obtain a finite amplitude of the hopping integral for the motion of the holon between two sublattices. (Note that in the summation of (2.22), $\mathbf{k} = 0$ has been removed excluding the b_0 component. Using (2.4), one can easily see that b_0 part has no contribution due to the sign in σ .) The mean field result remains approximately the same for the superexchange term H_J in which the holon position is fixed and $\eta_{\mathbf{k}}$ plays no role.

This hopping amplitude $B_0 \neq 0$ is consistent with $\Delta^s \neq 0$, and we may understand this in the following way. Physically, each spin subspace has a hidden local particle-hole symmetry, $b_{i\sigma} \rightarrow b_{i-\sigma}^\dagger$. It is exact and can be preserved in the RVB description if the no double occupancy constraint is strictly implemented locally. Let us assume that the holon is, say, at an odd sublattice site. Then, on performing a transformation $b_{i\sigma} \rightarrow b_{i-\sigma}^\dagger$ only in the *corresponding spin subspace*, it is easy to see that B_{ij}^0 at the hopping bond transforms into the RVB order parameter Δ^s . Note that at the mean-field level in SBMFT, the local hard-core constraint is relaxed where the particle-hole symmetry is no longer exact. But it can be checked that the symmetry $\eta_{\mathbf{k}\sigma} \rightarrow -\text{sgn}(\xi_{\mathbf{k}})\eta_{\mathbf{k}\sigma}$ in SBMFT still approximately corresponds to $b_{i\sigma} \rightarrow b_{i-\sigma}^\dagger$ at the global level according to (2.20) (It would be exact if $|u_{\mathbf{k}}| = |v_{\mathbf{k}}|$). It tells us that the direct hopping term for the holon indeed originates from local RVB spin pairing with a particle-hole symmetry in each spin subspace.

With $B^0 \neq 0$, G_h in the first line of (2.19) may be written, in the limit of $E \rightarrow -\infty$, as

$$G_h(E \rightarrow -\infty) \approx \sum_{\{c\}} g_h^c \left\langle e^{i \sum_c \hat{\phi}} \right\rangle_{\text{half-filling}} \quad (2.23)$$

where $g_h^c = 2^K \langle \hat{S}_c \rangle_{\text{half-filling}}$. Note that in $E \rightarrow -\infty$ limit $G_J \rightarrow 1/E$ becomes commutable with $e^{i\hat{\phi}}$. We can now calculate the phase string average $\langle e^{i \sum_c \hat{\phi}} \rangle_{\text{half-filling}}$ explicitly as

$$\begin{aligned} \left\langle e^{i \sum_c \hat{\phi}} \right\rangle_{\text{half-filling}} &= e^{i \langle \sum_c \hat{\phi} \rangle} \left\langle e^{i \sum_c (\hat{\phi} - \langle \hat{\phi} \rangle)} \right\rangle \\ &= e^{i \mathbf{k}_0 \cdot (\mathbf{r}_i - \mathbf{r}_j)} e^{-\frac{1}{2} \langle [\sum_c (\hat{\phi} - \langle \hat{\phi} \rangle)]^2 \rangle} \quad , \end{aligned} \quad (2.24)$$

where $\langle [\sum_c (\hat{\phi} - \langle \hat{\phi} \rangle)]^2 \rangle = \frac{\pi^2}{2} \langle (\sum_i^c : S_i^z :)^2 \rangle$, and $: S_i^z := S_i^z - \langle S_i^z \rangle$. Using the results for $\langle S_i^z S_j^z \rangle$ from SBMFT [24], one finds in the large $|\mathbf{r}_{ij}|$ limit, the asymptotic form for expression (2.24) and thus, the holon propagator as

$$G_h(j, i; E) \sim e^{i \mathbf{k}_0 \cdot (\mathbf{r}_i - \mathbf{r}_j)} e^{-\frac{|\mathbf{r}_i - \mathbf{r}_j|}{\lambda_L}} \quad . \quad (2.25)$$

The localization length is determined numerically, for the case $E = -\infty$, as $\lambda_L(E = -\infty) \sim 2.2a$ for \mathbf{r}_{ij} parallel to the x- or y-axis (Here, a is the lattice constant).

The exponential decay (2.25) of the holon propagator, *a typical characterization of localization phenomenon*, is fundamentally different from the power-law decay for the propagator generally expected when the hole behaves like a well-defined quasiparticle. The very fact that the holon propagator behaves like (2.25) as $E \rightarrow -\infty$ is enough to invalidate conventional quasiparticle behavior. As in conventional localization problems, we expect $\lambda_L(E)$ to increase with the energy E and to represent the true localization length scale at $E \geq E_G$ (E_G is the ground-state energy). Later, we shall determine the localization length $\lambda_L(E)$ numerically, in the physical regime of E . We find it to be generally larger than the overall scales of sample sizes ($< 6a \times 6a$) used in exact-diagonalization calculations. So, the hole localization caused by the phase string effect cannot be directly detected by exact diagonalization, owing to the limitation of the sample size. On the contrary, as in conventional localization problems, a localized electron can be mistaken for a delocalized electron simply because the sample sizes are smaller than the localization length. Thus, we argue that the well defined quasiparticle peak seen in finite size calculations is an artifact of small sample sizes and cannot persist at scales beyond λ_L .

III. SPECTRAL FUNCTION

A. Effective theory

As pointed out earlier, the bosonic spin RVB pairing gives an extremely good description of the undoped antiferromagnet for *both* short-range and long-range spin-spin correlations. The direct hopping of the holon originates from *short-range* RVB pairing with a local particle-hole symmetry. Unlike the long-range spin correlations, the short-range correlations are not sensitive to doping and the local RVB order parameter Δ^s provides a certain local “rigidity” that underpins the doped antiferromagnet, as long as the the average spacing between the holes is larger than the distance between nearest neighbors. Indeed, such a direct hopping term can persist into the metallic (superconducting) phase at finite doping, as discussed in Ref. [27]. However, unlike the metallic system, the one-hole case is different as we do not expect the AF spin background to change at thermodynamic scales. As discussed in the previous section, one may, to leading order, assume the spin background to be the same as that at half-filling. The feedback effect on the spin part at high-energy, short-distance scales will be considered in the Appendix.

In the previous section, we saw that the holon picks up the effect of the phase string and that the effective Hamiltonian can be written as

$$H_h = -t_h \sum_{\langle ij \rangle} e^{i\hat{\phi}_{ij}} f_i^\dagger f_j + h.c. \quad (3.1)$$

with $t_h = B^0 t \simeq 0.4t$. Here, the nontrivial effect arises solely from the phase $\hat{\phi}_{ij}$, reflecting the irreparable phase string effect. In terms of (2.14), we may rewrite

$$\begin{aligned} e^{i\hat{\phi}_{ij}} &= e^{i\mathbf{k}_0 \cdot (\mathbf{r}_i - \mathbf{r}_j)[1 - \sigma_{ij}]} \\ &\equiv e^{i\mathbf{k}_0 \cdot (\mathbf{r}_i - \mathbf{r}_j)} e^{-ia_{ij}} \end{aligned} \quad (3.2)$$

where

$$\mathbf{k}_0 = \left(\pm \frac{\pi}{2a}, \pm \frac{\pi}{2a} \right) \quad (3.3)$$

and $a_{ij} = \mathbf{k}_0 \cdot (\mathbf{r}_i - \mathbf{r}_j) [\sigma_{ij}]$.

To characterize the strength of a_{ij} , let us consider the gauge invariant quantity $\sum_{\square} a_{ij}$, *i.e.*, the fictitious “magnetic” flux seen by the holon hopping around a plaquette: $i \rightarrow i + \hat{x} \rightarrow i + \hat{x} + \hat{y} \rightarrow i + \hat{y} \rightarrow i$. One can easily get

$$\sum_{\square} a_{ij} = \pm \pi (S_{i+\hat{x}}^z + S_{i+\hat{x}+\hat{y}}^z - S_{i+\hat{y}}^z - S_i^z). \quad (3.4)$$

Generally, $\langle \sum_{\square} a_{ij} \rangle = 0$, and the strength of the quadratic fluctuations is given by

$$\langle (\sum_{\square} a_{ij})^2 \rangle = \pi^2 \left(1 - \frac{4}{3} \langle \mathbf{S}_i \cdot \mathbf{S}_{i+\hat{x}+\hat{y}} \rangle \right). \quad (3.5)$$

Using the SBMFT one can estimate $\sqrt{\langle (\sum_{\square} a_{ij})^2 \rangle} \approx 0.86\pi$ and find that, for two plaquettes separated far away from each other (*i.e.*, the distance $R_{12} \gg a$),

$$\langle (\sum_{\square} a_{ij})_1 (\sum_{\square} a_{lk})_2 \rangle \sim O\left(\frac{a^4}{R_{12}^4}\right). \quad (3.6)$$

Note that the spatial correlations between the fluxes threading through different plaquettes fall off rapidly in (3.6). This is because the contribution from the long-range AF fluctuations is strongly canceled out in (3.4). Similarly, the correlations of fluxes per plaquettes at different times also decay very quickly. Thus, as the first order of approximation one may treat a_{ij} as a gauge field describing random fluxes in the white-noise limit with the strength controlled by (3.5). (The phase string effect beyond the random flux approximation is briefly discussed in the Appendix in conjunction with the momentum dependence of the energy-integrated spectral function).

In the effective model (3.1), the effect from the longer-range spin correlations involving the AFLRO, which influence the hopping of the holon through (2.6), has been omitted. This process has been considered in the SCBA approach as the *sole* source assisting the holon hopping. In the following we reexamine it in the presence of the bare holon term

(3.1). With the Bose condensate $b_0 \neq 0$ (AFLRO), one may express $c_{i\sigma} \equiv (-\sigma)^i \bar{c}_{i\sigma} + (-\sigma)^i f_i^\dagger : b_{i\sigma} :$ with $\bar{c}_{i\sigma} = b_0 f_i^\dagger$ and $: b_{i\sigma} := b_{i\sigma} - b_0$. Then, Eq.(2.6) leads to the following hopping Hamiltonian,

$$H_h^{LSW} = -t \sum_{\langle ij \rangle \sigma} \sigma \left[\bar{c}_{i\sigma} : b_{j\sigma}^\dagger : f_j + f_i^\dagger : b_{i\sigma} : \bar{c}_{j\sigma}^\dagger \right] + h.c. \quad (3.7)$$

If there were no bare hopping (3.1) for the *holon*, H_h^{LSW} would represent a virtual process, which, by the SCBA treatment [7–10], would give rise to the well-known quasiparticle description for $\bar{c}_{i\sigma}$. But in the presence of (3.1), H_h^{LSW} literally describes the process for \bar{c}_σ (the “quasiparticle”) to *decay* into a holon-spinon pair. In this case, the propagator \tilde{G}_e for \bar{c}_σ will no longer behave like the one for a dressed quasiparticle found in SCBA. In contrast, to leading order approximation, it will be simply proportional to the propagator of $f_i^\dagger : b_{i\sigma} :$ to be discussed below. So in the following we do not consider H_h^{LSW} in (3.7) and simply switch $\bar{c}_{i\sigma}$ off, by assuming either the sample size to be large but finite or $T = 0^+$, such that $b_0 = 0$ without loss of generality.

B. Spectral function

In this subsection, we shall show that the main features observed in ARPES can be described within our formalism. We attribute the broad spectra that are observed to the fact that the physical electron is a convolution of spinon and holon excitations. We show that the dispersion of the photoelectron is governed by the dispersion of the spinon, and consequently, isotropic. We also show that the phase string plays a crucial role in causing the sharpest spectra at low binding energy locating at $(\pm\pi/2, \pm\pi/2)$ (*i.e.*, the “Fermi points”).

The single-electron propagator may be expressed in the following *decomposition* form

$$G_e \approx iG_b \cdot G_h \quad (3.8)$$

where

$$G_b(i, j; t) = -i(-\sigma)^{i-j} \left\langle T_t b_{i\sigma}(t) b_{j\sigma}^\dagger(0) \right\rangle, \quad (3.9)$$

and

$$G_h(i, j; t) = -i \left\langle T_t f_i^\dagger(t) f_j(0) \right\rangle. \quad (3.10)$$

Here we mainly focus on the properties of the spectral function defined by $A^e(\mathbf{k}, \omega) = -\frac{1}{\pi} \text{Im} G_e(\mathbf{k}, \omega) \text{sgn}(\omega)$, which can be measured by ARPES. Using the decomposition (3.8), one finds the convolution law

$$A^e(\mathbf{k}, \omega) = \theta(-\omega) \frac{1}{N} \sum_{\mathbf{k}'} \int_{\omega}^0 d\omega' \rho_h(\mathbf{k}' - \mathbf{k}, \omega' - \omega) \rho_b(\mathbf{k}', \omega') \quad (3.11)$$

at $T = 0^+$ where ρ_b and ρ_h are the spectral function corresponding to G_b and G_h , respectively.

By using (2.20) one can easily obtain

$$\text{Im} G_b = -\pi [u_{\mathbf{k}}^2 \delta(\omega - E_{\mathbf{k}}^s) - v_{\mathbf{k}}^2 \delta(\omega + E_{\mathbf{k}}^s)]. \quad (3.12)$$

As noted above, in the one-hole case this half-filling mean-field propagator should not be affected thermodynamically by the motion of the single holon. Then the corresponding electron spectral function is written as

$$A^e(\mathbf{k}, \omega) = \frac{1}{N} \sum_{\mathbf{k}'} v_{\mathbf{k}'}^2 \rho_h(\mathbf{k}' - \mathbf{k}, -E_{\mathbf{k}'}^s - \omega) \quad (3.13)$$

where the condition $\rho_h \neq 0$ only at $\omega \geq 0$ is used which defines the bottom of the holon band at $\omega = 0$.

The overall feature of $A^e(\mathbf{k}, \omega)$ versus ω is shown in Fig. 5 at different \mathbf{k} 's along $(0, 0)$ to \mathbf{k}_0 . The whole energy range of the spectral function is about $16J \approx 2.24eV$ (for $J = 0.14eV$). Here we have chosen $t_h = 2J$ ($t = 5J$) in (3.1) in obtaining the holon spectral function ρ_h which is calculated numerically by exactly diagonalizing H_h under random flux with $|\sum_{\square} a_{ij}| \leq 0.86\pi$ in the white noise limit. The sample size is 32×32 .

Even though not delta-function-like, the spectral function do show peaks which become sharper near both energy bottom and top as the momentum approaches \mathbf{k}_0 . According to (3.1), the bottom and top of the holon band are near

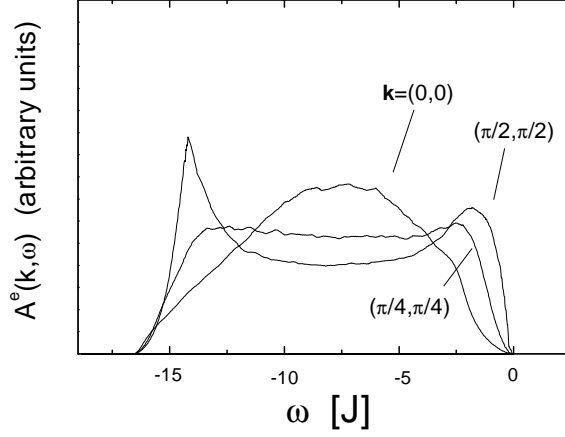


FIG. 5. The full shape of the spectral function calculated at $\mathbf{k} = (\pi/2, \pi/2)$, $(\pi/4, \pi/4)$, and $(0,0)$. Note the whole energy range extends over $16J \approx 2.24eV$ (for $t = 5J$, $J = 0.14eV$).

the momenta shifted away from $(0,0)$ and (π,π) , respectively, by \mathbf{k}_0 , where the spectral function ρ_h is sharpest in contrast to the broadest feature near the band center due to the random flux. On the other hand, the spinon spectrum $E_{\mathbf{k}}^s$ is maximum at \mathbf{k}_0 and vanishes at momenta $(0,0)$ and (π, π) . The convolution law of (3.11) then combines the contributions from the holon and spinon to result in Fig. 5. Note that the peaks are asymmetric at the top and bottom of the band. The effect of the spinon spectrum is most visible at lower binding energies, as will be further discussed below. A similar asymmetric structure in one-dimension has been found in Ref. [28].

Let us now focus on the structure of A^e at low binding energies in comparison with ARPES measurements on $\text{Sr}_2\text{CuO}_2\text{Cl}_2$ [1,2] and $\text{Ca}_2\text{CuO}_2\text{Cl}_2$ [3]. In the left panel of Fig. 6, we plot A^e within the energy range of $8J \simeq 1.1eV$ at \mathbf{k} positions along a line from $(0,0)$ to $(\pi/2, \pi/2)$ and then from $(\pi/2, \pi/2)$ to $(\pi, 0)$. The peak or edge position shows an isotropic dispersion along $(0,0)$ to $(\pi/2, \pi/2)$ and from $(\pi/2, \pi/2)$ to $(\pi, 0)$, consistent with the experiments. Such a dispersion has a bandwidth about $2J$ and is clearly correlated with the spinon spectrum $E_{\mathbf{k}+\mathbf{k}_0}^s$. The latter is marked by small bars at different \mathbf{k}' s where the position of the minimum $E_{\mathbf{k}+\mathbf{k}_0}^s$ at \mathbf{k}_0 is fixed around $\omega = 0.7J$ as a reference point. In the right panel of Fig. 6, a plot of A^e along $(0,0)$ and $(0,\pi)$ is shown where the peak is replaced by an edge which looks dispersionless, also in good agreement with the experiment. Indeed, a very flat (only about 13% change) $E_{\mathbf{k}+\mathbf{k}_0}^s$ along $(0,0)$ to $(0, \pi)$ is indicated in the figure by the small bars. In Fig. 7, the spinon spectrum $E_{\mathbf{k}+\mathbf{k}_0}^s$ fits the observed ARPES “quasiparticle” spectrum data reasonably well over the whole Brillouin zone along \mathbf{k}_0 (Σ) to $(0,0)$ (Γ) and $(0,\pi)$ (X) (which are symmetric in our theory) with $J = 0.14eV$. Note that the low-energy scale is determined by J instead of t and the features shown in Fig. 6 are not sensitive to t . Thus, second - or further neighbor hopping terms are not expected to play as important a role as they do in determining the energy bottom, $\epsilon_{\mathbf{k}}$, shown in Fig. 1.

The reason that the low energy peak or edge of the spectral function is correlated with the spinon spectrum can be easily understood by noting the fact that $\rho_h(\mathbf{k}, \omega)$ becomes the sharpest near the bottom $\omega = 0$ with $\mathbf{k} \approx \mathbf{k}_0$ which contributes to A^e in (3.13) at $\mathbf{k}' \approx \mathbf{k} + \mathbf{k}_0$ and $\omega \approx -E_{\mathbf{k}+\mathbf{k}_0}$. In Fig. 8(a), the spectral function along $(0,0) - \mathbf{k}_0$ is shown when the maximal strength of $|\sum_{\square} a_{ij}|$ is reduced from 0.86π to 0.1π . Here the correlation between the low-energy peak or edge positions and the spinon spectrum is even more apparent as the holon spectral function ρ_h becomes sharper near $\omega = 0$ and \mathbf{k}_0 . The evolution from a peak to an edge as \mathbf{k} moves away from \mathbf{k}_0 is because the spectral function of the holon is quickly broadened away from the band bottom in the presence of the random flux. Note that compared to the experiment the peak structure in Fig. 8(a) is a bit too sharp which implies that the actual strength of $|\sum_{\square} a_{ij}|$ should be closer to our estimation used in Fig. 6.

The line shape of the spectral function shown in Fig. 6 and Fig. 8(a) looks strikingly similar to the ARPES measurements in $\text{Sr}_2\text{CuO}_2\text{Cl}_2$ and $\text{Ca}_2\text{CuO}_2\text{Cl}_2$ [1–5]. It reflects essentially the *convolution* law of spinon and holon, i.e., the spin-charge separation. But we would like to point out that the simple convolution law is not enough. Here the *coherence* of the spinon in contrast to the *incoherent* holon is key to the characteristic features of the line shape and the “dispersion” of the peak or edge structure. To illustrate this point, we replace the coherent factor $v_{\mathbf{k}}^2$ in (3.13) by a constant (i.e., $v_{\mathbf{k}}^2 = 1$), and re-calculate the spectral function which is plotted in Fig. 8(b) along $(0,0) - \mathbf{k}_0$. One sees that the whole low-energy peak-edge feature in the left panel of Fig. 6 and Fig. 8(a) totally disappears in Fig. 8(b). In this case, the summation in (3.13) smears out the peak structure and A^e is more or less like the density

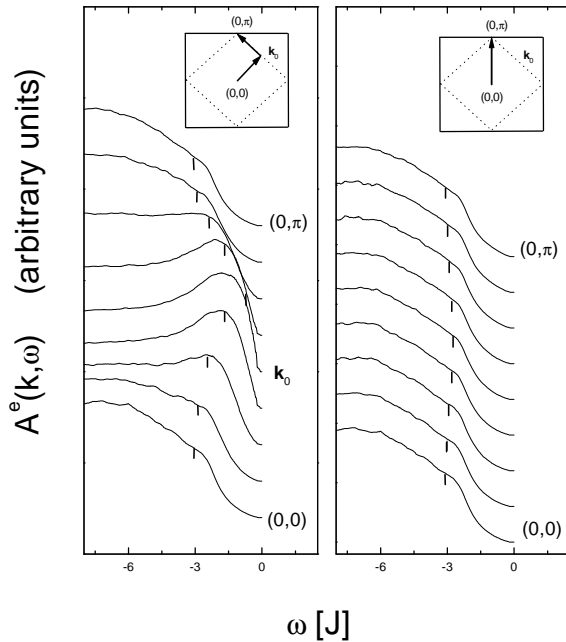


FIG. 6. The spectral function at low binding energy along different momentum scans. The small bars mark the spinon spectrum $E_{\mathbf{k}+\mathbf{k}_0}^s - \mu_0$ with $\mu_0 = 0.7J$.

of states for the holon. So the coherent factor v^2 in the spinon propagator is crucial for the “quasiparticle” peak to emerge in the spin-charge separation formulation of the spectral function, which is the unique result of the *bosonic* RVB description of spins. This explains why the correct line shape has not been directly obtained in the slave-boson formalism, even though the prediction that the “quasiparticle” spectrum obtained in ARPES actually corresponds to the spinon spectrum was first made [6] there.

The incoherence of the holon is also an important factor as discussed above. It is well-known that a particle must be generally localized, at least in the low-energy regime, in the presence of the random flux governed by H_h in (3.1). We have checked the localization lengths corresponding to the case of Fig. 6 using standard methods [29]. The localization length quickly jumps from 4-15 (in lattice units) to 36 – 50 near the holon band edge which covers an energy range related to the low-energy peaks of the spectral function in Fig. 6. As noted before, the localization length scale of the holon is generally much larger than the maximum sample sizes ($< 6 \times 6$) in numerical exact-diagonalization calculations [12]. Thus, numerical calculations providing a “metallic” quasiparticle picture should be irrelevant to the true picture at large length scales.

Finally, to conclude our discussion of ARPES in the Mott insulator, we turn to the experimental results of Ronning *et al.* [3]. These authors identify a “remnant Fermi surface” in the insulator from ARPES measurements: they define

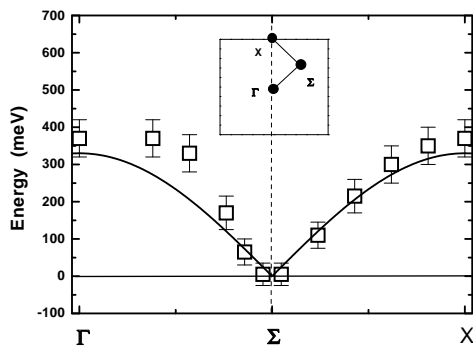


FIG. 7. The “quasiparticle” spectrum determined by the ARPES [3] (open square) and by the spinon spectrum $E_{\mathbf{k}+\mathbf{k}_0}^s$ (solid curve).

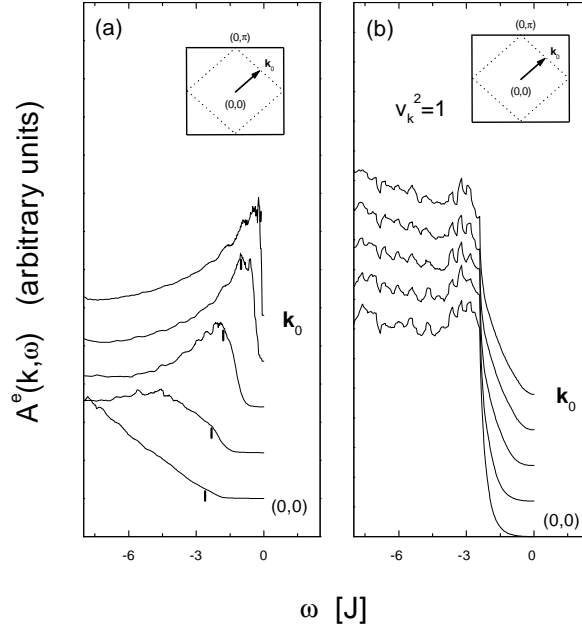


FIG. 8. (a) The spectral function similar to the left panel of Fig. 6, but with the random flux strength per plaquette reduced to 0.1π (see text). Small bars marked the same spinon spectrum as in Fig. 6 (but with $\mu_0 = 0.2J$); (b) The line shape of the spectral function in the left panel of Fig. 6 is greatly changed if the spinon coherent factor $v_{\mathbf{k}}^2$ is replaced by a constant 1.

the so-called relative momentum distribution

$$n_{\mathbf{k}}^r(\omega_0) = \int_{\omega_0}^0 \frac{d\omega}{\pi} A^e(\mathbf{k}, \omega) \quad , \quad (3.14)$$

with the cutoff energy $\omega_0 = -0.5eV$, then identify “ k_F ” by locating the position where $n_{\mathbf{k}}^r$ drops suddenly. Then a “remnant Fermi surface” is found as the contour of steepest descent of $n_{\mathbf{k}}^r$. Such a “remnant Fermi surface” roughly coincides with the large Fermi surface expected for a free electron gas at half-filling concentration. It should be emphasized that this contour is *not* an equal energy contour. In fact, the peak (or edge) of the spectral function disperses at momenta along the “remnant Fermi surface” as much as that shown in Fig. 7.

So the “remnant Fermi surface” mainly indicates a strong momentum dependence of the energy-integrated spectral function, $n_{\mathbf{k}}^r$. We believe this is due to the effect of the mobile hole on the spin background (at very short time scales). So far we have not considered the influence of the phase string effect on the spin degrees of freedom. This is based on the fact that a single hole does not affect the spin background at the thermodynamic scale. However, the AF background *surrounding* the doped hole should be still strongly distorted by the hopping at $t \gg J$, which in turn will feed back on the hole itself through the phase string effect. Obviously, this happens at short length and time-scales. Consequently, one has to go beyond the effective Hamiltonian (3.1) as well as the random flux treatment of the phase string effect. Not being within the main purview of this paper, we relegate the discussion of such effects to the Appendix.

IV. CONCLUSIONS AND DISCUSSIONS

Although antiferromagnetism in the Mott insulator has been well understood based on the bosonic RVB description, the problem of a single hole doped into such a system is found to be nontrivial. Unlike the spin-polaron picture in which the hole is predicted to behave like a Landau-Fermi quasiparticle carrying a finite-size spin distortion around it, the real picture for the motion of the doped hole is that it always picks up a string of signs from the spin background during its hopping, known as the phase string, which leads to the destruction of the “coherence” of the doped hole as a Landau-Fermi quasiparticle.

The phase string characterizes the effect of spin backflow during the motion of the hole. The irreparable nature of phase string is intimately related to spin-charge separation: the hole cannot carry a precise spin-1/2 quantum number

with it. In contrast, if the holon and spinon were tightly confined together, the phase string effect would become trivial (reparable), as is the case when one naively uses the c -operator to replace the spinon-holon decomposition in (2.3). Hence, the demonstration that the phase string effect cannot be “healed” through spin superexchange interaction at low energies, presented in Sec. IIB and Refs. [18,19], points directly to spin-charge separation. It is also found that the spin backflow, or equivalently, the phase string leads to mutual statistics between the hole and spin degrees of freedom. That the backflow of spin current could lead to mutual statistics and spin-charge separation was also anticipated by Baskaran [30].

In the one-hole case, the phase string effect mainly acts on the holon part, causing its localization. But the spinon remains coherent in the bosonic RVB background. Consequently, during its propagation, a bare hole releases the coherent spinon constituent whose isotropic dispersion essentially determines the position of the low-energy peak or edge of the spectral function. On the other hand, spin-charge separation characterized by the convolution law of the holon and spinon propagators is responsible for the intrinsic broad feature of the spectral function at higher energy. In the phase string formalism, the singular part of the phase string effect also decides the Fermi points \mathbf{k}_0 in the low-energy, long-time limit as well as the large “remnant Fermi surface” structure in the high-energy, equal-time limit. We thus obtain a systematic and natural explanation for the ARPES measurements within the framework of the $t-J$ model. Conversely, one may say that the ARPES experiments have clearly presented evidence for spin-charge separation, as emphasized by Anderson.

We find that the “coherence” of the spinon, reflected by the factor $v_{\mathbf{k}}^2$ in SBMFT, plays an important role in determining the ARPES line shapes. A naive convolution without this factor is not enough to explain the line shape observed by ARPES. We also note that the strong temperature dependence of the ARPES line shapes over a wide energy range [31], may be easily understood based on the temperature dependence of $v_{\mathbf{k}}^2$. Details will be presented elsewhere. Finally, we point out that the temperature dependence of $v_{\mathbf{k}}^2$ is also crucial to get the correct behavior of the relaxation rate ($1/T_1$) in nuclear magnetic resonance measurements, spin-spin correlation length, and other magnetic properties at half-filling within the SBMFT.

The prediction that the holon as the charge carrier is localized by the phase string effect is also consistent with the cuprate superconductors. It is known that the phase with AFLRO (weakly doped regime) is always an insulator. According to our theory, the localization is due to the intrinsic nature of the doped Mott insulator instead of external reasons like the Anderson localization in the presence of impurities.

Note that the localization of the hole is because the phase string is solely picked up by the hole, and the antiferromagnetic background remains the same as at half-filling, thermodynamically. At finite density of holes, both spin and charge degrees of freedom will be affected by the phase string, which can lead to a metallic (superconducting) phase [27] without AFLRO. We emphasize that the irreparable phase string effect always exists, even in the metallic phase. This is because the phase string reflects the competition between the hopping and superexchange interactions in the $t-J$ model, which has nothing to do with the existence of AFLRO. Thus, the phase string effect will persist at any finite doping so long as short range antiferromagnetic correlations persist [19,27].

ACKNOWLEDGMENTS

We acknowledge useful discussions with A. Ferraz, T. Tohyama, T. K. Lee, and especially C. Kim and F. Ronning who kindly provided their experimental data. We also thank Barry Wells for discussions on ARPES and useful correspondence. Work at Houston was supported in part by Texas ARP No.3652707, the Robert A. Welch foundation, and TCSUH. V.N.M. is supported by NSF Grant DMR-9104873.

APPENDIX A: SHORT TIME SCALE EFFECTS AND THE “REMNANT FERMI SURFACE”

The holon is localized by phase string in space. But at a short scale within the localization length, the holon may behave like in the metallic phase at finite doping where holons are mobile. It has been found [19,27] that in the metallic phase the phase string effect will influence both the spin and charge degrees of freedom in such a way that the correct decomposition form for the electron becomes

$$c_{i\sigma} = h_i^\dagger \bar{b}_{i\sigma} e^{i\hat{\Theta}_{i\sigma}^{string}}, \quad (\text{A1})$$

where h_i^\dagger and $\bar{b}_{i\sigma}$ are the “true” holon and spinon operators and the phase shift field $e^{i\hat{\Theta}_{i\sigma}^{string}}$ precisely keeps track of the non-reparable phase string effect. In the following we will use this formalism to describe the local, high-energy regime in the one-hole case and show a nontrivial consequence of the phase string effect.

In the one-hole case, the phase shift field can be written as $e^{i\hat{\Theta}_{i\sigma}^{string}} = (-\sigma)^i e^{\frac{i}{2}\Phi_i^b}$ in which

$$\Phi_i^b = \sum_{l \neq i} \text{Im} \ln (z_i - z_l) \left(\sum_{\alpha} \alpha n_{l\alpha}^b - 1 \right). \quad (\text{A2})$$

with $z_i = x_i + iy_i$ representing the complex coordinate of a lattice site i and $n_{l\alpha}^b$ denoting the spinon number at site l .

In order to understand n_k^r , let us first take ω_0 to $-\infty$. In this high-energy or equal-time limit, n_k^r reduces to the momentum distribution n_k which is given by

$$\begin{aligned} n_k &= \frac{1}{N} \sum_{ij} e^{i\mathbf{k} \cdot (\mathbf{r}_j - \mathbf{r}_i)} \langle c_{j\sigma}^\dagger c_{i\sigma} \rangle \\ &= \frac{1}{N} \sum_{ij} e^{i\mathbf{k} \cdot (\mathbf{r}_j - \mathbf{r}_i)} \left\langle \bar{b}_{j\sigma}^\dagger h_j \left(e^{i \int_{\Gamma} d\mathbf{r} \cdot \hat{\mathbf{A}}^f(\mathbf{r})} \right) h_i^\dagger(0) \bar{b}_{i\sigma} \right\rangle, \end{aligned} \quad (\text{A3})$$

in which the following expression for the equal-time phase-string factor is used:

$$e^{i\frac{1}{2}\Phi_i^b(t)} e^{-i\frac{1}{2}\Phi_j^b(0)} \Big|_{t \rightarrow 0^-} = e^{i \int_{\Gamma} d\mathbf{r} \cdot \hat{\mathbf{A}}^f(\mathbf{r})} \quad (\text{A4})$$

with

$$\hat{\mathbf{A}}^f(\mathbf{r}) = \frac{1}{2} \sum_l \left[\sum_{\sigma} \sigma n_{l\sigma}^b - 1 \right] \frac{\hat{\mathbf{z}} \times (\mathbf{r} - \mathbf{r}_l)}{|\mathbf{r} - \mathbf{r}_l|^2} \quad (\text{A5})$$

where the path Γ connects two lattice sites i and j without crossing other lattice sites. Clearly, in the equal-time limit, the momentum structure will be mainly decided by the oscillation of the phase string factor given in (A4).

For the one-hole case, n_k in (A3) is actually trivial and featureless ($= 1/2$). This is because $\langle c_{i\sigma}^\dagger c_{j\sigma} \rangle = \delta_{ij} \langle \bar{b}_{i\sigma}^\dagger \bar{b}_{i\sigma} \rangle$ using the non-double-occupancy constraint in which no propagation of the holon at a finite distance can occur at strictly equal time on the half-filling ground state. On the other hand, n_k^r for a finite cutoff ω_0 will involve a finite-time holon propagation over some finite distance. In this case, the phase string factor in (A4) will show up to determine the basic feature while the rest of the propagator involving holon and spinon will mainly give rise to a broadening in the momentum space depending on how far the holon and spinon constituents can travel under the cutoff ω_0 . At $\omega_0 = -\infty$, the momentum broadening would reach infinity (as only $i = j$ contributes) such that any momentum structure arising from $e^{i \int_{\Gamma} d\mathbf{r} \cdot \hat{\mathbf{A}}^f(\mathbf{r})}$ gets smeared out. But at a large but finite $|\omega_0|$ the momentum structure due to the phase string factor should show up. Here as an approximation the equal-time phase string factor is still used so long as $|\omega_0|$ is sufficiently large.

In the spin channel, a line-integral expression similar to (A4) also appears [32] in the spin-spin correlation function, leading to the so-called incommensurate antiferromagnetic peaks. Here we can borrow the similar method used in Ref. [32] to manipulate the contribution of the phase string factor (A4) in n_k^r , which gives rise to four ‘‘incommensurate peaks’’ at $(\pm\pi\kappa, 0)$ and $(0, \pm\pi\kappa)$ in momentum space with $\kappa \sim 1$ [33]. If this oscillating factor solely decides the momentum structure of n_k^r with the rest term in the propagator mainly contributing a broadening as discussed above, then one gets a contour plot of n_k^r in Fig. 9 in terms of the superposition of aforementioned four peaks (with $\kappa = 0.75$) at an arbitrary broadening (which is presumably controlled by the energy cutoff ω_0 : when $\omega_0 \rightarrow -\infty$, the broadening in the momentum space should go to infinity such that $n_k = 1/2$). Note that the values of n_k^r here are only meant for *relative* comparison.

We see that the overall feature is in qualitative agreement with the experimental data [3] whose one quarter portion is also shown in the inset of Fig. 9 for comparison. Here we remark that experimental data [34,35] of n_k^r seem to be photon-energy dependent, indicating the effect of the electron-photon matrix element, and there also exists controversies [34,35] on whether the ‘‘remnant Fermi surface’’ defined near the sharpest drop of n_k^r in \mathbf{k} -space is meaningful or not. But in the present approach the momentum dependence of n_k^r does not represent any real Fermi surface structure of the Mott antiferromagnet at half-filling. It only reflects the superposition of four peaks near $(\pm\pi, 0)$ and $(0, \pm\pi)$, an enhancement entirely coming from the dynamic effect of the doped hole as the result of a careful handling of the phase string effect in the local, high-energy regime. As a prediction, if experimentally $|\omega_0|$ is taken to sufficiently higher energy, the momentum dependence of n_k^r should get weaker and weaker and eventually $n_k^r \rightarrow n_k = 1/2$ at $\omega_0 \rightarrow -\infty$.

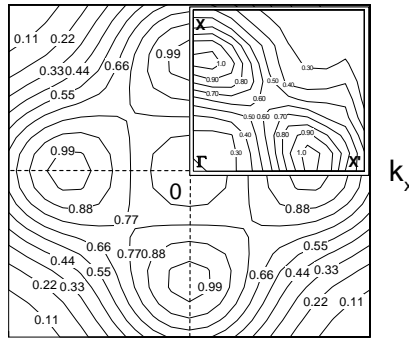


FIG. 9. The contour plot of the electron momentum distribution exhibiting a “remnant Fermi surface” structure. The experimental data [3] are shown in the insert at the upper right corner.

- [1] B.O. Wells, Z.-X. Shen, A. Matsuura, D.M. King, M.A. Kastner, M.Greven, and R.J. Birgeneau, Phys. Rev. Lett. **74**, 964 (1995).
- [2] C. Kim, P.J. White, Z.-X. Shen, T. Tohyama, Y. Shibata, S. Maekawa, B.O. Wells, Y.J. Kim, R.J. Birgeneau, and M.A. Kastner, Phys. Rev. Lett. **80**, 4245 (1998).
- [3] F. Ronning, C. Kim, D.L. Feng, D.S. Marshall, A.G. Loeser, L.L. Miller, J.N. Eckstein, I. Bozovic, Z.-X. Shen, Science, **282**, 2067 (1998).
- [4] S. LaRosa, I Vobornik, F. Zwick, H. Berger, M. Grioni, G. Margaritondo, R. J. Kelley, M. Onellion, and A. Chubukov, Phys. Rev. B **56**, R525 (1997).
- [5] C. Durr, S. Legner, R. Hayn, S.V. Borisenko, Z. Hu, A. Theresiak, M. Knupfer, M. S. Golden, J. Fink, F. Ronning, Z.-X. Shen, H. Eisaki, S. Uchida, C. Janowitz, R. Muller, R.L. Johnson, K. Rossnagel, L. Kipp, and G. Reichardt, cond-mat/0007283.
- [6] R.B. Laughlin, Phys. Rev. Lett. **79**, 1726 (1997); J. Phys. Chem. Solids. **56**, 1627 (1995).
- [7] S. Schmitt-Rink *et al.* Phys. Rev. Lett. **60**, 2793 (1988).
- [8] C. L. Kane, P.A. Lee, and N. Read, Phys. Rev. B **39**, 6880 (1989).
- [9] G. Martinez and P. Horsch, *ibid*, B **44**, 317 (1991).
- [10] Z. Lui and E. Manousakis, *ibid*, B **44**, 2414 (1991).
- [11] see, E. Dagotto, Rev. Mod. Phys. **66**, 763 (1994) and references therein.
- [12] P.W. Leung and R.J. Gooding, Phys. Rev. B **52**, R15711 (1995).
- [13] T.K. Lee and C.T. Shih, Phys. Rev. B **55**, 5983 (1997).
- [14] A. Nazarenko *et al.*, Phys. Rev. B **51**, 8676 (1995); R. Eder *et al.*, Phys. Rev. B **55**, R3414 (1997).
- [15] G. B. Martins, R. Eder, and E. Dagotto, Phys. Rev. B **60**, R3716 (1999).
- [16] T. Tohyama, Y. Shibata, S. Maekawa, Z.-X. Shen, and N. Nagaosa, J. Phys. Soc. Jpn, **69**, 9 (2000) and references therein.
- [17] P. W. Anderson, *The theory of superconductivity in the high- T_c cuprates*, Princeton University Press, 1997.
- [18] D. N. Sheng, Y. C. Chen, and Z. Y. Weng Phys. Rev. Lett. **77**, 5102 (1996).
- [19] Z. Y. Weng, D. N. Sheng, Y. C. Chen, and C. S. Ting, Phys. Rev. B **55**, 3894 (1997).
- [20] Here $(-\sigma)^i$ is introduced for convenience, which explicitly keeps track of the Marshall sign [21].
- [21] W. Marshall, Proc. Roy. Soc. (London) A **232**, 48 (1955).
- [22] S. Liang, B. Doucot and P. W. Anderson, Phys. Rev. Lett. **61**, 365 (1988).
- [23] Y. -C. Chen and K. Xiu, Phys. Lett. A **181**, 373 (1993).
- [24] D.P. Arovas and A. Auerbach, Phys. Rev. B **38**, 316 (1988); A. Auerbach, *Interacting Electrons and Quantum Magnetism* (Springer-Verlag, New York, 1994).
- [25] For convenience, the magnetization here is to lie in the $x - y$ plane instead of along the z -axis as in Ref. [8].
- [26] Note that such a hole-position-dependent choice of the phase $\eta_{k\sigma}$ is perfectly legitimate as in the sub-Hilbert-space in which the hole position is given, the commutation relations of b , b^\dagger remain unchanged. On the other hand, the spin-hole states are simply orthogonal if the hole is at different sites.
- [27] Z. Y. Weng, D. N. Sheng, and C. S. Ting, Phys. Rev. Lett. **80**, 5401 (1998); Phys. Rev. B **59**, 8943(1999).
- [28] H. Suzuura and N. Nagaosa, Phys. Rev. B **56**, 3548 (1997).
- [29] see, D. N. Sheng and Z. Y. Weng, Europhys. Lett. **50**, 776 (2000).
- [30] G. Baskaran, Prog. Theor. Phys. Suppl. **107**, 49 (1992).
- [31] C. Kim, F. Ronning, A. Damascelli, D.L. Feng, Z.-X. Shen, B.O. Wells, Y.J. Kim, R.J. Birgeneau, M.A. Kastner, L.L. Miller, H. Eisaki, and S. Uchida, preprint.
- [32] Z. Y. Weng, D. N. Sheng, and C. S. Ting, Phys. Rev. B **59**, 11367(1999).
- [33] Readers are referred to Ref. [32] for the detail, where a similar phase-string factor appearing in the spin-spin correlation function is discussed which gives rise to incommensurate shifts by $(\pm 2\pi\delta\bar{\kappa}, 0)$, etc., from (π, π) with δ denoting the doping

concentration and $\bar{k} \sim 1$.

[34] S. Hafner, D. M. Brammerier, C. G. Olson, L. L. Miller, and D. W. Lynch, cond-mat/0006366.

[35] F. Ronning, C. Kim, K. M. Shen, N. P. Armitage, A. Damascelli, D. H. Lu, Z.-X. Shen, and L. L. Miller, cond-mat/0007252.